THE JOURNAL OF PHYSICAL CHEMISTRY B

Article

pubs.acs.org/JPCB

Low-Temperature Spectroscopic Properties of the Peridinin–Chlorophyll *a*–Protein (PCP) Complex from the Coral Symbiotic Dinoflagellate *Symbiodinium*

Dariusz M. Niedzwiedzki,*[,†,‡] Jing Jiang,[†,§] Cynthia S. Lo,[†,§] and Robert E. Blankenship[†,‡]

[†]Photosynthetic Antenna Research Center, Washington University in St. Louis, St. Louis, Missouri 63130, United States

[‡]Departments of Biology and Chemistry, Washington University in St. Louis, St. Louis, Missouri 63130, United States

[§]Department of Energy, Environmental & Chemical Engineering, Washington University in St. Louis, St. Louis, Missouri 63130, United States

ABSTRACT: The spectroscopic properties of the peridinin–chlorophyll *a*–protein (PCP) from the coral symbiotic dinoflagellate *Symbiodinium* have been characterized by application of various ultrafast optical spectroscopies including femto- and nanosecond time-resolved absorption and picosecond time-resolved fluorescence (TRF) at 77 K. Excited state properties of peridinin and Chl *a* and their intramolecular interaction characteristics have been obtained from global fitting analysis and directed kinetic modeling of the data sets and compared to their counterparts known for the PCP from *Amphidinium carterae*. The lifetimes of the excited state of peridinin show close agreement with those known for the counterpart PCP, demonstrating that molecular interactions have the same characteristics in both complexes. More variances have been recorded for the excited state properties of Chl *a* including elongation of both the intramolecular energy transfer time between Chl's within the pair in the protein monomer and the excited state lifetime of the long wavelength form of Chl *a* (terminal acceptor). Kinetic modeling of formation of the peridinin triplet state has shown that the PCP is protected from potential photodamage due to an extremely fast peridinin triplet state formation of k_{TT} = (14.4 ± 2.3) × 10^9 s^{-1} ((70 ± 12)$^{-1}$ $(ps)^{-1}$) that guarantees instantaneous depletion of Chl *a* triplets and prevents formation of harmful singlet oxygen ($^1\Delta_gO_2$).

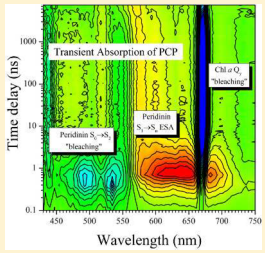

INTRODUCTION

Symbiodinium is a large group of endosymbiotic dinoflagellates that typically reside in the endoderm of corals. The endosymbiotic alga supplies corals with necessary nutrients that cannot be easily filtered out from nutrient-deficient marine environments in which most of the corals live. Recently, a severe reef disease known as coral bleaching became present in many places worldwide.[1,2] It is believed that bleaching is related with decrease or complete loss of *Symbiodinium* cells in the coral endoderm and in most cases is triggered by elevated water temperature. Recent studies of nonthermally resistant *Symbiodinium* species demonstrated that the alga's weak resistance against moderate irradiance at elevated water temperature is associated with the permanent loss of a large pool of two light-harvesting complexes associated with its photosystem II: peridinin–chlorophyll *a*–protein (PCP) and Chl *a*–Chl c_2–peridinin–protein complex (acpPC).[3] An acpPC is a membrane-bound protein, while PCP is a water-soluble complex that resides in the lumen of the thylakoid membrane and its interaction with photosystem II or with acpPC is still not understood.

PCP, unlike the majority of light-harvesting complexes, employs the carotenoid peridinin (Per) as the main photosynthetic pigment. The molecular structure of the PCP from the nonsymbiotic dinoflagellate phytoplankton *Amphidinium carterae*, well-known for its toxicity due to producing powerful ichthyotoxins and hemolytic substances,[4] was determined by Hofmann et al.[5] and to date several high-resolution crystal structures of different PCP forms, including native, refolded, mutated, so-called "high salt", and reconstituted with various Chl's and bacterio-Chl's, are available.[5−8] The molecular structure of the main form PCP (MFPCP) from *Amphidinium carterae* obtained with 2.0 Å resolution using X-ray crystallography revealed a trimeric structure made up of 32 kDa protein subunits. Each subunit contains eight noncovalently bound Per's and two Chl *a* molecules in a near C_2 symmetrical arrangement. The Per's are structured into two groups of four molecules grouped around each Chl *a* in van der Waals contact with the π-electron system of the Chl *a* macrocycle. The center-to-center distance between two Chl *a* molecules within a subunit is 17.4 Å.[5] The specific molecular arrangement in the PCP antenna complex very effectively facilitates intermolecular transfer of energy of absorbed photons. Previous studies demonstrated that the efficiency of Per-to-Chl *a* energy transfer is near 100%.[9,10]

Recent studies of the PCP from *Symbiodinium* sp. CS-156 revealed that the strain possesses the monomeric form of the complex with a molecular weight of 32.7 kDa. The sequence alignment of *Symbiodinium* sp. CS-156 and *Amphidinium*

Special Issue: Rienk van Grondelle Festschrift

Received: January 29, 2013
Revised: April 1, 2013
Published: April 4, 2013

carterae (PDB ID: 1PPR) PCPs shows ~83% similarity and conserved pigment binding sites. The pigment stoichiometry in both PCPs is preserved. The molecular structure of the PCP from *Symbiodinium* is still not determined; however, based on significant similarities in the protein sequence and pigment stoichiometry, the PCP complexes from both dinoflagellates may have similar structures.[5,11]

So far, only basic spectroscopic properties of *Symbiodinium* sp. CS-156 PCP have been studied. These include steady-state absorption and fluorescence spectroscopy performed at room temperature and at 77 K.[11] In this work, we expand knowledge about properties of the PCP complex from *Symbiodinium* by applying transient optical spectroscopic methods, including nanosecond and femtosecond time-resolved absorption and picosecond time-resolved fluorescence. The results directly enhance our insight into pigment interaction within the complex and help understand if PCP may be involved in the process of coral bleaching. The spectroscopic results are also compared with those reported previously for the MFPCP complex from *Amphidinium carterae*.

MATERIALS AND METHODS

Protein and Pigment Purification and Basic Spectral Characterization. PCP complexes were obtained from *Symbiodinium* sp. CS-156 cells as described in Jiang et al.[11] The pigments were separated from a methanol extract of the pelleted PCP using an Agilent 1100 HPLC system employing a reverse phase column Zorbax Eclipse XDB-C18 (250 mm × 4.6 mm). Peridinin was separated using acetonitrile as a mobile phase with 1.5 mL min^{-1} flow rate. Chl *a* was separated using the method described earlier.[12] Low temperature measurements of Per and Chl *a* were performed in 2-methyltetrahydrofuran (2-MTHF). For 77 K measurements (steady-state and time-resolved), the concentrated PCP was resuspended in 10 mM Tris−HCl (pH 8.0) containing 50% glycerol (v/v). All the experiments were performed at 77 K using a Janis VNF-100 liquid nitrogen cryostat (Janis Research Company, MA, USA). Steady-state absorption spectra were recorded using a Shimadzu 1800 spectrophotometer. Steady-state fluorescence of the PCP was obtained using a Photon Technology International fluorometer. Emission and excitation monochromator slits were set to a bandpass of 4 nm and corrected for response of the detector. Fluorescence was monitored at right angle with respect to excitation. The PCP sample was excited at 530 nm. In order to mimic the protein natural environment, all measurements on the PCP were performed in air-saturated buffer.

Femtosecond Time-Resolved Transient Absorption Spectroscopy. Time-resolved pump−probe absorption experiments were carried out using Helios, a femtosecond transient absorption (TA) spectrometer (Ultrafast Systems, LCC) coupled to a femtosecond laser system described in detail previously.[13] The PCP sample was excited at the Per absorption band at 530 and 490 nm and at the Chl *a* Q_y band at 670 nm. In order to eliminate Chl *a* singlet excited state annihilation effects within the protein scaffold, the energies of the pump beam were set to 60, 80, and 400 nJ/pulse, respectively, in a spot size of 1 mm diameter corresponding to an intensity of (0.19−1.7) × 10^{14} photons/cm^2 per pulse.

Picosecond Time-Resolved Fluorescence Spectroscopy. Time-resolved fluorescence experiments were carried out using a universal streak camera from Hamamatsu consisting of a cooled N51716-04 streak tube, C5680 blanking unit, digital CCD camera (Orca2), slow speed unit M5677, C10647, and C1097-05 delay generators and an A6365-01 spectrograph from Bruker. Excitation pulses (at 530 nm) were produced by an ultrafast optical parametric oscillator (OPO) Inspire100 from Radiantis-Spectra-Physics pumped with a Mai-Tai ultrafast Ti:sapphire laser generating ~90 fs laser pulses at 820 nm with a frequency of 80 MHz. After the OPO, the repetition rate of the excitation beam was lowered to 4 MHz, consisting of a 250 ns time gap between subsequent excitations (it was assumed that potential accumulation of either Per or Chl *a* triplets will have a negligible influence on the overall fluorescence signal). An excitation beam with a power of ~10 mW was focused on the sample in a circular spot of ~2 mm diameter, which corresponds to a photon intensity of ~1 × 10^{10} photons/cm^2 per pulse.

Nanosecond Time-Resolved Transient Absorption Spectroscopy. Triplet-minus-singlet (T−S) spectra of Per in the PCP were taken using an Edinburgh Instruments LP920-K/S flash photolysis spectrometer equipped with a Hamamatsu R2658 photomultiplier detector (kinetic mode) and Andor ICCD camera (IStar with DH720-18H-13 CCD head) (spectral mode) that was described in detail elsewhere.[12] The sample was excited at 530 nm with a photon density of ~10^{16} photons/cm^2 per pulse. Transient absorption signals were averaged from 50 to 100 times in order to obtain a satisfactory quality of either kinetic trace or T−S spectra. Sample integrity was checked by taking steady-state absorption spectra before and after the experiment.

Transient Absorption Data Processing and Global Fitting. Group velocity dispersion of the TA spectra was corrected using Surface Xplorer 2.0 (UltrafastSystems LCC) by building a dispersion correction curve from a set of initial times of transient signals obtained from single wavelength fits of the representative kinetics. Global fitting of the data sets was performed using a modified version of ASUfit, a program provided by Dr. Evaldas Katilius at Arizona State University (http://www.public.asu.edu/~laserweb/asufit/asufit.html). The full width at half-maximum of the instrument response function was obtained as one of the global fitting parameters and was less than 250 fs. Global fitting was done by applying a sequential irreversible decay path model (A → B → C → D → ...). The spectral profiles obtained from this fitting of the TA data sets are termed evolution associated difference spectra (EADS).[14] Derivative equations modeling the rise of the Per triplets in the PCP were solved using Matlab R2009b (MathWorks, Inc., USA).

RESULTS

Steady-state absorption and fluorescence spectra of the PCP complex from *Symbiodinium* sp. CS-156 are shown in Figure 1.[11] The spectrum consists of absorptive bands associated with two pigments: carotenoid Per and Chl *a*. The broad band between 450 and 570 nm originates from the sum of the $S_0(1^1A_g^-) \rightarrow S_2(1^1B_u^+)$ transitions of eight Per's. The narrow peaks visible at ~435 and 666 nm are Soret and Q_y bands of Chl *a*. The PCP fluorescence spectrum represents fluorescence from Chl *a* with a strong main (0−0) band at ~669 nm (~70 cm^{-1} Stoke's shift) and a weaker (0−1) vibronic band at ~728 nm. Even though the overall $S_0(1^1A_g^-) \rightarrow S_2(1^1B_u^+)$ band of Per's in the PCP is not well-resolved at ultralow temperatures, the positions of absorption spectra of individual molecules were assigned in the case of the PCP from *Amphidinium carterae*,[6,10] and a similar approach has been employed in these studies.

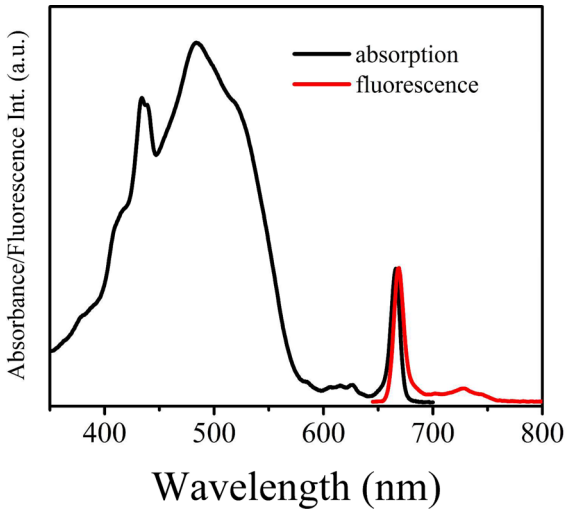

Figure 1. Steady-state absorption and fluorescence spectra of the PCP from *Symbiodinium* sp. CS-156. The spectra were taken at 77 K and are normalized at the Q_y band of Chl *a*.

Figure 2 shows the results of spectral reconstruction of the absorption spectrum of the PCP shown in Figure 1. The

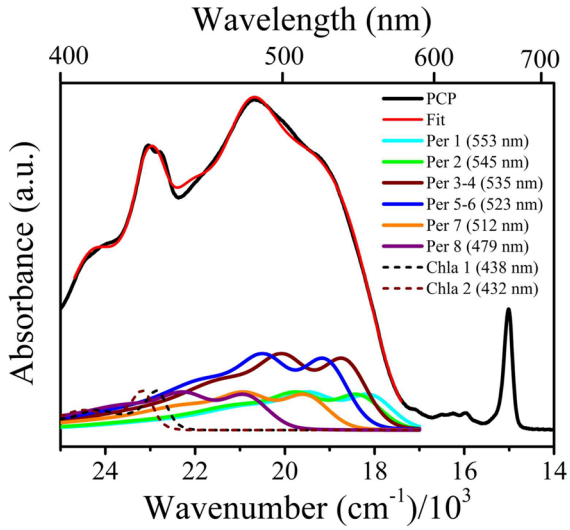

Figure 2. Reconstruction of the 77 K absorption spectrum of the PCP from individual spectra of Chl *a* and Per taken at 77 K in 2-MTHF. The fitting model assumed that the PCP protein contains two Chl *a* and eight Per molecules. Positions of the absorption spectra of individual components are listed in the graph. Detailed information about the fitting procedure is given in the main text.

reconstruction was obtained as follows. First, in order to avoid distorting effects of the nonlinearity of the wavelength scale, wavelengths were converted to wavenumbers. Then, an automated fitting procedure (implemented in Origin software) was applied. The fitting employed a user-defined multivariable equation mimicking the sum of spectra of eight individual Per's and two Chl *a*'s (molecular ratio conserved) taken at 77 K in 2-methyl-tetrahydrofuran (2-MTHF). The fitting assumed that amplitudes of the absorption spectra of the components are constant and identical (contribute equally) but positions may vary. The fit obtained from the fitting appears to be quite adequate; however, it also has deficiencies in some spectral ranges. These might be caused by small differences between real (but unknown) absorption spectra of individual pigments in the protein scaffold and those taken in 2-MTHF.

Therefore, one can question how appropriate is a choice of absorption spectra of individual pigments used for spectral reconstruction. The polar character of Per binding pockets in the PCP from *Amphidinium carterae* was confirmed by the presence of the ICT state, also at 77 K.[9] This should cause a polarity-induced increase of the number of conformational isomers of Per, each of which will exhibit a slightly different absorption spectrum. The spectra summed together would produce a broad, almost featureless, absorption band.[15] However, it is uncertain that the rigid protein backbone of the PCP will allow formation of many conformational isomers such as happens in polar solvents. Also, it is impossible to find an answer by simply analyzing the PCP absorption spectrum because the broad and featureless collective absorption band of Per's does not change much even at 77 K. However, the TA experiments of the PCP from *Amphidinium carterae* performed at 77 K show that bleaching of the ground state absorption band of excited Per's has well-resolved vibronic bands. Comparative studies (not shown) have shown that bleaching of Per ground state absorption in the PCP can be very adequately mimicked by the absorption spectrum taken in 2-MTHF at 77 K. The results of fitting are somewhat different from the counterparts obtained for the MFPCP from *Amphidinium carterae*[10] and are discussed in detail later.

Figure 3 shows results of TRF of Chl *a* in the PCP complex. The excitation wavelength was set at 530 nm (Per), which prevented direct excitation of potentially unbound Chl *a*. The two-dimensional fluorescence contour is given in Figure 3A. The *Z*-axis represents photon counts (see legend for color code). The TRF spectra presented in Figure 3B were obtained by summation of individual spectra in the temporal ranges 0−1 ns (red line) and 10−18 ns (black line). The spectra practically do not differ from each other as well from steady-state fluorescence shown in Figure 1. This suggests that spectral equilibration of fluorescence occurs on the sub-nanosecond time scale and cannot be resolved. The representative fluorescence kinetic trace extracted from the data set is given in Figure 3C. The fit (red line) obtained by using a monoexponential decay function gave a fluorescence lifetime of Chl *a* in the PCP of 7.4 ns.

Femtosecond time-resolved absorption spectra of the PCP obtained upon excitation of the Q_y band of Chl *a* (670 nm) are shown in Figure 4. The representative TA spectra are shown in Figure 4A.

These are taken at different delay times with respect to the time of the excitation. They consist of multiple positive and negative spectral features. The most intense are two negative bands at 436 and 670 nm associated with depletion of the pool of Chl's in an electronic ground state due to excitation and are proportional to the number of molecules being excited. The spectral profile should simply represent an inverted steady-state absorption spectrum of this portion of the molecules. It is also known that, for Chl *a* at low temperatures, amplitudes of Soret and Q_y bands are similar.[10] However, in the spectra presented here, "bleaching" of the Q_y band is ∼2 times more intense than Soret. The anomaly can be simply explained by the presence of stimulated emission from Chl *a* driven by the probe light. In this case, stimulated emission will match the spontaneous fluorescence presented in Figure 1 and this is a reason why it can be barely distinguished from pure "bleaching". However, since the probe light also contains photons with energy

dx.doi.org/10.1021/jp401022u | J. Phys. Chem. B 2013, 117, 11091−11099

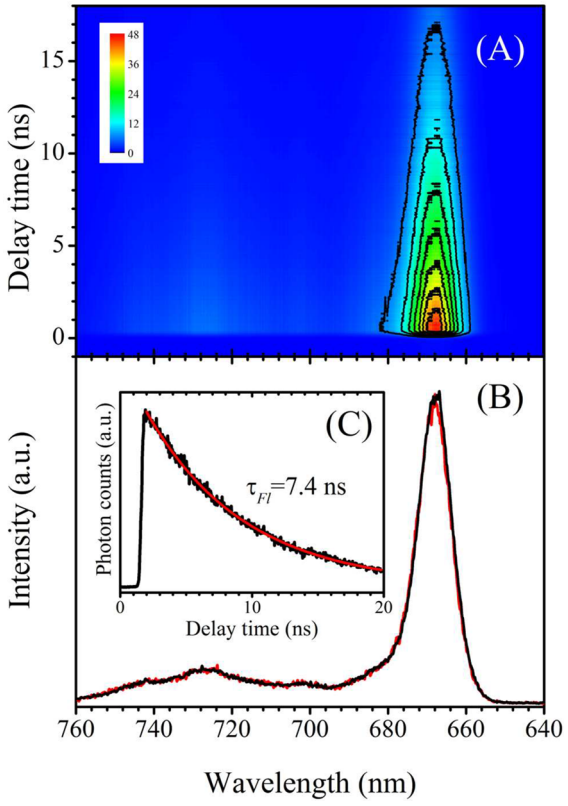

Figure 3. (A) Time-resolved fluorescence profile of the PCP obtained at 77 K by streak camera. The protein was excited at 530 nm (Per band). The color barcode represents the number of counted photons. (B) Time-resolved fluorescence spectra obtained by summation of the elementary spectra between 0 and 1 ns (red) and 10 and 18 ns (black). (C) Representative fluorescence kinetic trace extracted from the data set presented in part A. The red line represents the fit done by the monoexponential decay function. The fluorescence lifetime of Chl *a* in the PCP obtained from this fitting is 7.4 ns.

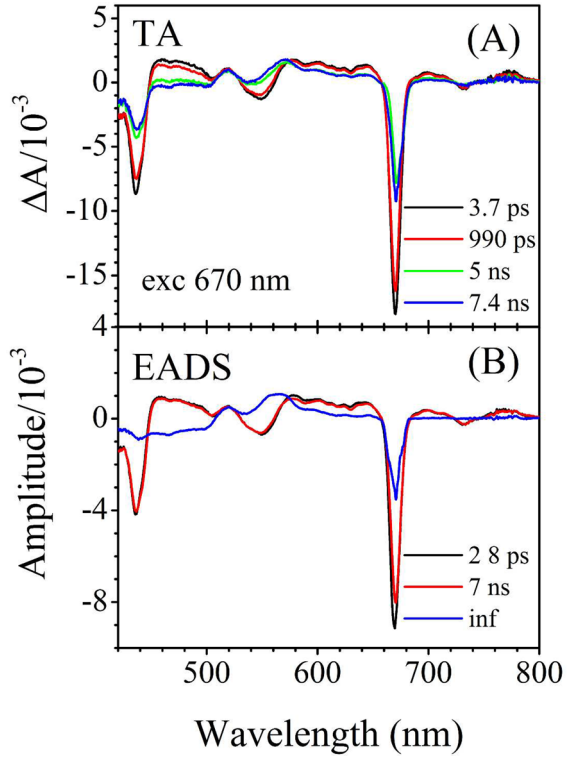

Figure 4. (A) Time-resolved transient absorption spectra of the PCP recorded at different delay times upon excitation at 670 nm (Chl *a*). (B) Global fitting results (EADS) of the TA data set. The spectra were recorded at 77 K.

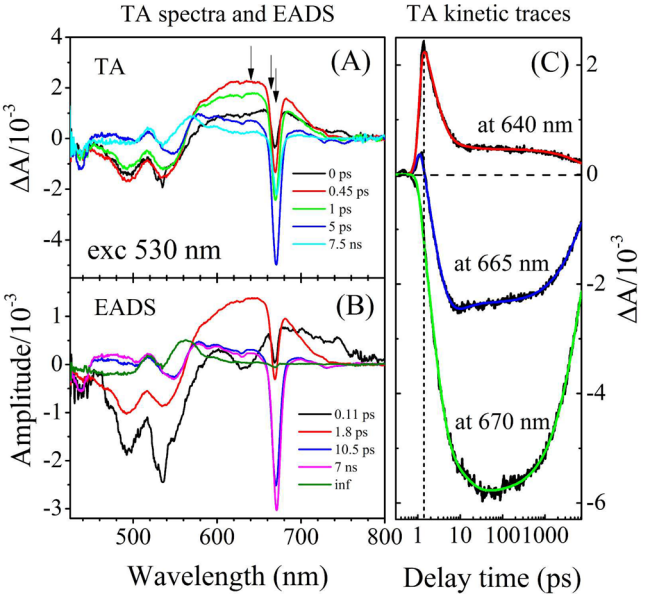

Figure 5. (A) Time-resolved transient absorption spectra of the PCP recorded at 77 K at various delay times upon excitation at 530 nm (Per). (B) Global fitting results (EADS) of the TA data set and (C) representative kinetic traces accompanied with fits from global fitting. The wavelengths on which the kinetic traces were probed are indicated by arrows. The vertical dashed line marks the delay time at which the ICT/S_1 → S_n transition reaches amplitude.

matching to the (0−1) vibronic band of spontaneous fluorescence, this spectral feature should also be visible. Indeed, it is present in the spectra as the small dip at ∼730 nm. Another distinct feature is revealed in the spectral range between 500 and 570 nm. It has a wavy shape and is known to be not associated with Chl's and originates from electroabsorption (Stark effect) of neighboring Per's.[6] The spectral profile between 500 and 600 nm evolves over time and after a few nanoseconds reveals a clear signature of the T−S spectrum of Per sensitized by the triplet state of Chl *a*.[16]

Figure 5 presents the results of time-resolved absorption of the PCP taken upon excitation at 530 nm. Selection of this wavelength guarantees selective excitation of spectral forms of Per contributing to the absorption spectrum of the PCP on the long wavelength edge of the collective absorption band. The early time TA spectra recorded between 420 and 800 nm (Figure 5A) reveal a transient band associated with the excited state absorption (ESA) of Per, manifested as a broad positive feature between 560 and 750 nm. Simultaneously, very prominent bleaching of the ground state absorption of Per is visible with two noticeable vibronic peaks at 492 nm (0−1) and 535 nm (0−0). The ESA of Per decays within a few picoseconds and gives rise to bleaching of Chl *a* ground state absorption. The TA spectra taken at later delay times are consistent with those recorded for the PCP excited into the Q_y band of Chl *a*. The results of global fitting of the TA data set from Figure 5A are shown in Figure 5B. The fitting required five kinetic components. The first EADS with a time constant

dx.doi.org/10.1021/jp401022u | J. Phys. Chem. B 2013, 117, 11091−11099

of 0.11 ps with a typical spectral signature of pronounced bleaching of the $S_0(1^1A_g^-) \rightarrow S_2(1^1B_u^+)$ absorption and ESA band extended in the NIR range represents decay of the Per $S_2(1^1B_u^+)$ excited state. A small dip coinciding with the Q_y band of Chl *a* visible in this EADS is a signature of Per−Chl *a* energy transfer via the $S_2(1^1B_u^+)$ state. The 0.11 ps EADS decays to form EADS with a lifetime of 1.8 ps, with spectral shape characteristic for the ESA associated with the ICT/S_1 state of Per. It is believed that the intrinsic lifetime of the ICT/S_1 state of Per in the PCP is ∼16 ps;[17] thus, the observed significant shortening demonstrates very efficient Per-to-Chl *a* energy transfer. The next EADS profiles with lifetimes of 10.5 ps and 7 ns are clearly associated only with Chl *a*.

Evolution from 10.5 ps EADS to 7 ns EADS reveals a shift in the Q_y band position and is additionally coupled with the simultaneous rise of bleaching at the long wavelength side of the collective Q_y band. The infinite (on this scale) EADS represents the decay of the triplet state of Per and is identical with that obtained upon excitation into the Q_y band of Chl *a* (Figure 4B). The representative kinetic traces extracted from the TA data set, accompanied by fits from global fitting, are given in Figure 5C. The wavelengths of extractions are also indicated by arrows in Figure 5A. For clarity of view, the time scale was expressed in logarithmic notation. The dashed line represents the time delay at which the Per ESA reaches amplitude. The traces clearly demonstrate that the decay of bleaching of the Q_y band of "blue" Chl *a* (665 nm trace) is associated with rise of bleaching of the Q_y band of "red" Chl *a* (670 nm trace) and can be interpreted as intramolecular energy transfer within the pair of Chl's in the core of the PCP monomer.

The TA and global fitting results of the PCP excited at 490 nm are given in Figure 6. The results of spectral reconstruction (Figure 2) clearly indicate that this excitation should stimulate all spectral forms of Per within the PCP.

However, unlike for the 530 nm excitation, in this case, it should also be possible to resolve the contribution from two so-called "blue" Per's (denoted as Per 7 and 8 in Figure 2). However, comparison of the TA data obtained from both excitations reveals practically no differences. The only one that is visible is flattening of the Per ESA band in the 590−650 nm range. However, this change does not affect the excited state lifetime. Also, bleaching of the ground state absorption does not differ from that observed for 530 nm excitation. This is strong evidence that an extremely fast energy transfer takes place between Per's within a time range shorter than their $S_2(1^1B_u^+)$ state lifetime; therefore, within a few tens of femtoseconds, the excitation is already relocated on the "red" Per's.

Figure 7 shows properties of the Per triplet state in the PCP that is formed via a sensitization process by the triplet state of Chl *a*. Figure 7A demonstrates the rise of the $T_1 \rightarrow T_n$ transient band, monitored at 560 nm within the first few nanoseconds (temporal window of spectrometer) after excitation into the Per band (530 nm) (the kinetic trace is extracted from the data set shown in Figure 5A).

Because the absorbed energy is rapidly transferred into Chl's in the core of the PCP, this wavelength selection will prevent direct excitation and formation of triplet states of Chl's that are potentially present in the sample but are not bound into the complex. The Per triplet decay is shown in Figure 6B. Fitting performed using a monoexponential decay function gave a quite adequate fit with a triplet decay lifetime of 18.9 μs. This

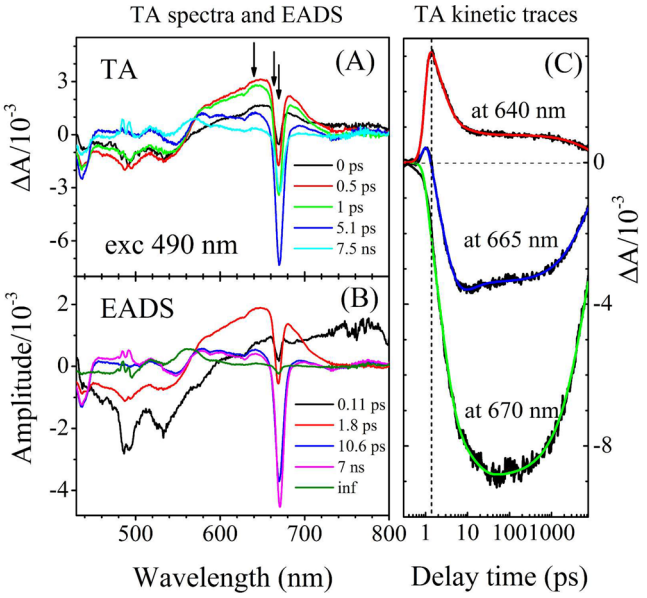

Figure 6. (A) Time-resolved transient absorption spectra of the PCP recorded at 77 K at various delay times upon excitation at 490 nm (Per). (B) Global fitting results (EADS) of the TA data set and (C) representative kinetic traces accompanied with fits from global fitting. The wavelengths on which kinetic traces were probed are indicated by arrows. The vertical dashed line marks the delay time at which the ICT/$S_1 \rightarrow S_n$ transition reaches amplitude.

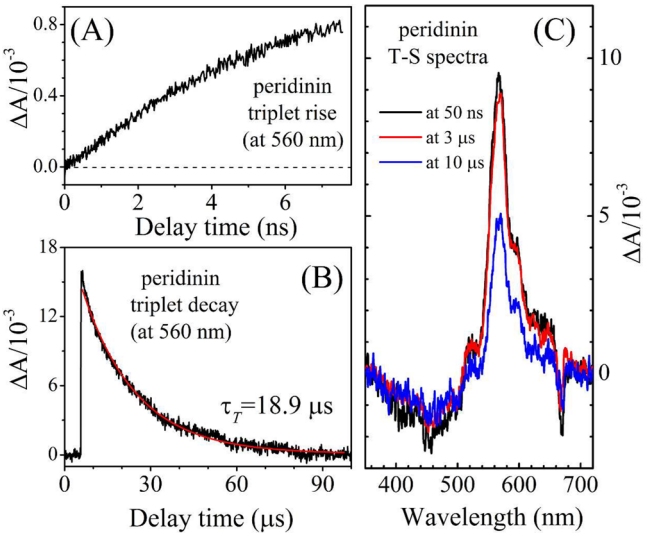

Figure 7. Spectral and temporal characteristic of the triplet state of Per in the PCP at 77 K: (A) rise of the $T_1 \rightarrow T_n$ transient absorption band; (B) decay of the triplet state of Per in the PCP; (C) the T−S transient absorption spectra of Per in the PCP taken at different delay times with respect to the excitation. The strong, narrow $T_1 \rightarrow T_n$ band has the maximum located at 567 nm.

value lies in the middle of the range of values obtained for Per either in solvents or in the PCP complexes (see Table 1).

Certainly, the kinetic trace of the rise of the Per triplet shown in Figure 7A does not reflect the microscopic rate of triplet formation but the overall evolution of the concentration of Per's in the triplet state.

Even though the rise of the Per triplet was previously recorded using time-resolved FTIR,[22] detailed analysis of Chl *a*-Per triplet−triplet transfer in the PCP complex has not been

dx.doi.org/10.1021/jp401022u | J. Phys. Chem. B 2013, 117, 11091−11099

Table 1. Triplet State Lifetimes of Per in Various Environments[a]

environment	τ_T (μs)	method	temp	ref
n-hexane	5.5	TA	RT	16
acetonitrile	6	TA	RT	16
PCP (A)	10	T-R FTIR	RT	18
PCP (A)	13, 42	T-R FTIR	RT	19
PCP (A)	10	T-R FTIR	RT	18
PCP (A, H)	13, 58	TA	2−200 K	20
PCP (A)	13, 40	T-R FTIR	77 K	18
PCP (A)	50 ($\tau_{1/2}$ = 35)[b]	T-R FTIR	100 K	21
PCP (S)	18.9	TA	77 K	this study

[a]TA, transient absorption; T-R FTIR, time-resolved FTIR; RT, room temperature; A, *Amphidinium carterae*; H, *Heterocapsa pygmeae*; S, *Symbiodinium*. [b]$\tau_{1/2}$ provided in the literature source.

performed. The TA data of the PCP obtained in this study in sub-nanosecond and nanosecond time scales show very good temporally resolved rise of the Per triplet and provide the opportunity to calculate accurately the rate of Chl *a*−Per triplet−triplet transfer. In order to obtain the rate, the following kinetic scheme should be considered:

$$\begin{array}{ccccc} {}^1\mathrm{Chl}^* & \xrightarrow{k_{isc}} & {}^3\mathrm{Chl} & \xrightarrow{k_{TT}} & {}^3\mathrm{Per} \\ \downarrow k & & \downarrow k_{TChl} & & \downarrow k_{TPer} \\ {}^1\mathrm{Chl} & & {}^1\mathrm{Chl} & & {}^1\mathrm{Per} \end{array} \quad (1)$$

where $k_F = k + k_{isc}$ is the rate constant of excited singlet state decay of Chl *a*, k_{isc} is the rate constant of intersystem crossing for Chl *a*, k_{TT} is the rate constant of the Chl *a*−Per triplet−triplet transfer, k_{TChl} is the rate constant of decay of Chl *a* triplet, and k_{Tper} is the rate constant of decay of Per triplet. The scheme can be mathematically described as follows:

$$\frac{d[^3\mathrm{Chl}]}{dt} = k_{isc}\cdot[^1\mathrm{Chl}^*] - k_{TT}\cdot[^3\mathrm{Chl}] - k_{TChl}\cdot[^3\mathrm{Chl}]$$
$$\frac{d[^3\mathrm{Per}]}{dt} = k_{TT}\cdot[^3\mathrm{Chl}] - k_{TPer}\cdot[^3\mathrm{Per}] \quad (2)$$

Since contributions of the last terms in both equations are negligible in the first few nanoseconds after excitation, the equations can be simplified to

$$\frac{d[^3\mathrm{Chl}]}{dt} = k_{isc}\cdot[^1\mathrm{Chl}^*] - k_{TT}\cdot[^3\mathrm{Chl}]$$
$$\frac{d[^3\mathrm{Per}]}{dt} = k_{TT}\cdot[^3\mathrm{Chl}] \quad (3)$$

The initial pool of Chl *a* molecules Chl_0^* being in the singlet excited state is practically instantaneously (within a few picoseconds) populated via energy transfer from excited Per, and it can be assumed that $[^1\mathrm{Chl}^*] = \mathrm{Chl}_0^*\cdot e^{-k_F t}$, $[^3\mathrm{Chl}]_{t=0} = 0$, and $[^3\mathrm{Per}]_{t=0} = 0$ (no triplets of either Chl's or Per's at the time of excitation). The equations have the following solutions:

$$[^3\mathrm{Chl}] = \frac{\mathrm{Chl}_0^*\cdot k_{isc}}{(k_F - k_{TT})\cdot e^{k_{TT}\cdot t}} - \frac{\mathrm{Chl}_0^*\cdot k_{isc}}{(k_F - k_{TT})\cdot e^{k_F\cdot t}}$$
$$[^3\mathrm{Per}] = \frac{\frac{\mathrm{Chl}_0^*\cdot k_{isc}}{e^{k_{TT}\cdot t}} - \frac{\mathrm{Chl}_0^*\cdot k_{isc}\cdot k_{TT}}{k_F\cdot e^{k_F\cdot t}}}{k_F - k_{TT}} - \frac{\mathrm{Chl}_0^*\cdot k_{isc}}{k_F} \quad (4)$$

The last equation can be applied to fit the kinetic trace given in Figure 7A. First, in order to perform fitting, the ΔA at 560 nm must be converted to the actual molecular concentration of Per's in the triplet state in the sample. That can be simply done according to the Beer−Lambert law: $\Delta A_T = \varepsilon_T\cdot C\cdot l$ (ΔA, change of absorbance at 560 nm; C, molar concentration; l, optical path (1 cm); ε_T, molar extinction coefficient of triplet). The value of ε_T is unknown; however, it can be easily deduced from the mutual proportion between the triplet transient band and accompanied bleaching of the ground state absorption band in the T−S spectrum that is shown in Figure 7C. For the ground state absorption of Per, a molar extinction coefficient in methanol was used (ε = 86 L mM^{-1} cm^{-1} at 470 nm).[23] Since for Chl *a* in the PCP significant overlap of ground state absorption bleaching and stimulated emission is observed, the value of Chl_0^* is difficult to define and it was left as an adjustable parameter in the fitting procedure. The k_{isc} value was assumed to be 0.085 × 10^9 s^{-1}, the same as for Chl *a* measured previously in ether at room temperature.[24] The k_F was defined to be 0.135 × 10^9 s^{-1} (reciprocal of fluorescence lifetime, 7.4 ns). The results of fitting of eq 4 to the kinetic trace data are shown in Figure 8. The output parameters obtained from fitting

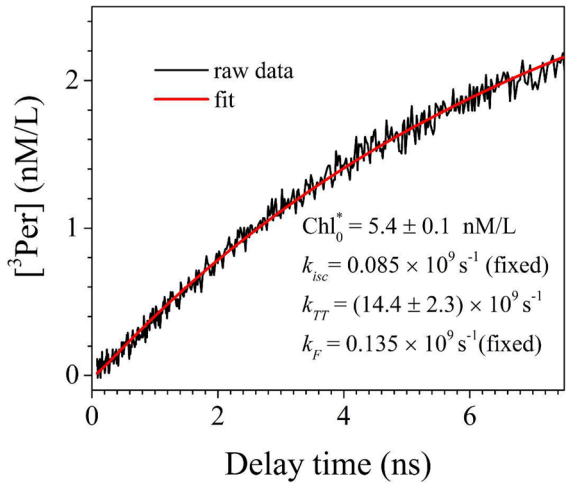

Figure 8. Evolution of the concentration of the Per pool being in the triplet state accompanied by a simulated curve (red) obtained from applying eq 4. The values of constant (known) parameters were marked as fixed. See the main text for parameter descriptions.

are k_{TT} = (14.4 ± 2.3) × 10^9 s^{-1} (or (70 ± 12)$^{-1}$ (ps)$^{-1}$) and Chl_0^* = 5.4 nM/L. It is clear that a large disproportion between k_{TT} and k_{isc} leads to the situation in which the population of the triplet state of Chl *a* is practically virtual (rate of depletion is much faster than rate of population) and the PCP shows no accumulation of potentially dangerous Chl *a* triplets.

DISCUSSION

Similarities and Differences between the PCPs from *Symbiodinium* and *Amphidinium carterae*. Spectroscopic properties of the PCP from *Amphidinium carterae* have been extensively studied since its molecular structure was published in the 1990s.[5] The properties of singlet excited states of the bound pigments and their molecular interactions have been explored by a broad range of advanced spectroscopic techniques like femtosecond time-resolved absorption after two-[25] and one-photon excitation,[9,10,26−29] four-wave-mixing spectroscopy,[30] two-photon absorption,[31] and time-resolved

dx.doi.org/10.1021/jp401022u | J. Phys. Chem. B 2013, 117, 11091−11099

fluorescence[32,33] and have been simulated using theoretical models[18,31,34−36] and reviewed.[7,17,37] Complementary studies were performed at cryogenic temperatures and could be used for comparison purposes.[9,10,27] Reconstruction of the 10 K absorption spectrum of the MFPCP from *Amphidinium carterae* employing 10 K absorption spectra of Per in 2-MTHF done by Ilagan et al.[10] revealed that the spectrum can be satisfactorily simulated if the spectra of two Per's are significantly blue-shifted ("blue" Per's) relative to the others which could be grouped into three spectrally different pairs ("red" Per's). A very similar pattern is also observed in the PCP from *Symbiodinium* with one alteration. The longest wavelength pair of Per's is split into two components differing by 8 nm. However, the overall difference between absorption spectra of the complexes may be difficult to justify due to the different approaches used in fitting protocols. However, no difference has been observed in the effective lifetime of the ICT/S_1 state of Per (1.7 ps in PCP from *Amphidinium carterae* vs 1.8 ps in PCP from *Symbiodinium*).

However, noticeable discrepancies appear in the case of the properties of Chl *a*. The global fitting analysis performed in these studies shows that the effective lifetime of the short wavelength absorbing Chl *a* is 10.5 ps in comparison to 5.5−6.8 ps obtained for the PCP from *Amphidinium carterae*. The difference may illustrate a slightly different packing of Chl's in both complexes and could originate from either an elongated intramolecular distance and/or mutual orientation of macrocycles. The largest difference is observed in the lifetime of long-wavelength absorbing Chl *a*. The studies performed for the PCP from *Amphidinium carterae* revealed a lifetime ranging between 2 and 4.5 ns (77 K, RT data),[25−27] a number that is substantially smaller than 7−7.4 ns measured in the PCP from *Symbiodinium*. The observed shortening of lifetime of the final Chl *a* acceptor may be associated with slow phase annihilation of Chl *a* excited states occurring between PCP trimers even at low excitation intensities, as it was pointed out by van Stokkum et al.[27] Because the PCP from *Symbiodinium* exists largely in a monomeric conformation, the process mentioned above will not occur. It is very probable that differences observed either in basic spectroscopic properties or excited state dynamics (singlet and triplet) in PCP complexes from various dinoflagellates are practically negligible and originate from nonunified methodologies (different temperatures, fitting models, exciting laser intensities, etc.) used to perform experiments and analyze spectroscopic data.

Peridinin Triplet State Formation in the PCP. Triplet state dynamics of Per in the native (main form) MFPCP and (high salt) HSPCP from *Amphidinium carterae* has been studied by various techniques including time-resolved step-scan FTIR,[19,21] optically detected magnetic resonance (ODMR) and time-resolved EPR,[38−42] and nanosecond time-resolved absorption.[18,26] As mentioned before, we are not aware of any detailed analysis of the rise of the concentration of Per triplets in the PCP. Thus, the k_{TT} rate constant value could be compared only with analogous analysis performed for the rate of formation of carotenoid (presumably lutein) triplet in the solubilized LHCII from spinach done by Schödel et al.[43] On the basis of kinetic modeling, the authors concluded that k_{TT} is $\geq 2 \times 10^9$ s^{-1} (500 ps)$^{-1}$ but very likely is $\leq 10 \times 10^9$ s^{-1} (100 ps)$^{-1}$. The value of $(14.4 \pm 2.3) \times 10^9$ s^{-1} $(70 \pm 12)^{-1}$(ps)$^{-1}$ for Per in the PCP obtained in this study demonstrates that the rate of formation of the carotenoid triplet state in the PCP exceeds the expectation that could be drawn from LHCII. This is more evidence as to how ideally molecular arrangement, intramolecular interaction, and environmental protein are suited in the PCP in order to maintain both light absorption supporting and photoprotective properties of Per at the highest possible level.

The ODMR and time-resolved EPR techniques demonstrated that in the PCP from *Amphidinium carterae* two Per's, denoted as 624 and 614 in the crystal structure[5] are the main acceptors of the Chl *a* triplet.[19,40,41] These results are in agreement with suggestions that Per 614 has the strongest coupling with Chl *a*.[6,27,34,35,44,45] Moreover, recent time-resolved FTIR studies have clearly shown that triplets of Per and Chl *a* coexist.[19,46] Gall et al.[47] based on comparative studies have suggested that carotenoid−Chl *a* triplet sharing is a common feature of all LHC complexes from algae and higher plants and represents an adaptation of the molecular mechanism of photoprotection against photooxidative stress. Thus, based on this rule, it is expected that triplet sharing between Per and Chl *a* also takes place in the PCP from *Symbiodinium*. The T−S spectrum presented in Figure 7C shows bleaching of the Chl *a* Q_y band that coexists with the Per $T \rightarrow T_n$ transition for its entire lifetime, suggesting that indeed the triplet is delocalized over both molecules. However, this is not a decisive proof; similar spectral features in a T−S spectrum are observed also for BChl *a* in LH complexes from various purple bacteria[48] in which it is associated with changes of the closest dielectric caused by carotenoid triplet.[47] It is also impossible to determine precisely if the Per triplet is localized on one or two Per molecules because most resolved vibronic bands in the ground state spectrum bleaching of Per (Figure 7C) are centered at 535 nm and this position matches very well to two Per's having the same spectral signature (see the reconstruction of the absorption spectrum of the PCP shown in Figure 2). It could only be hypothesized that these two, spectrally identical Per's in the PCP from *Symbiodinium* would be analogous to Per624 and Per614 in the PCP from *Amphidinium carterae*.

CONCLUSIONS

The fact that the PCP from *Symbiodinium* differs from its *Amphidinium carterae*'s counterpart in the apoprotein sequence by 17% does not significantly influence the spectroscopic properties of the protein bound pigments. The lifetimes of the excited state of Per show almost ideal agreement with those known for the PCP from *Amphidinium carterae*, demonstrating that molecular interactions have the same characteristics in both complexes. More variances are observed for excited state properties of Chl *a*. Elongation of the intramolecular energy transfer time between Chl's within the pair in the protein monomer suggests that the distance between interacting Chl's and their reciprocal orientation can be different. Detailed analysis of the formation of the Per triplet state shows that the PCP is exceptionally well protected from potential photodamage. Extremely fast Per triplet state formation of $k_{TT} = (14.4 \pm 2.3) \times 10^9$ s^{-1} $((70 \pm 12)^{-1}$ $(ps)^{-1})$ guarantees instantaneous depletion of Chl *a* triplets (^{3}Chl *a*). This completely inhibits the formation of harmful singlet oxygen ($^1\Delta_g O_2$) that is formed via sensitizing its triplet ground state ($^3\Sigma_g^- O_2$) by the Chl *a* excited triplet state.[49−51] Thus, permanent loss of a large population of the PCP antenna observed in the thermally nonresistant *Symbiodinium* species upon moderate irradiance conditions[3] cannot be simply explained by a weak photodamage resistance of this complex.

dx.doi.org/10.1021/jp401022u | J. Phys. Chem. B 2013, 117, 11091−11099

Since the protein shows very high photodamage resistance, other factors that can control complex population have to be taken under consideration in order to explain the phenomenon.

AUTHOR INFORMATION

Corresponding Author

*Address: Photosynthetic Antenna Research Center, Washington University in St. Louis, St. Louis, MO 63130, Campus Box 1138, USA. Phone: +1 (314) 935-8483. Fax: +1 (314) 935-4925. E-mail: niedzwiedzki@wustl.edu.

Notes

The authors declare no competing financial interest.

ACKNOWLEDGMENTS

This material is based upon work supported as part of the Photosynthetic Antenna Research Center (PARC), an Energy Frontier Research Center funded by the U.S. Department of Energy, Office of Science, Office of Basic Energy Sciences, under Award No. DE-SC 0001035.

REFERENCES

(1) Hoegh-Guldberg, O. Climate Change, Coral Bleaching and the Future of the World's Coral Reefs. *Mar. Freshwater. Res.* **1999**, *50*, 839−866.

(2) Glynn, P. W. Coral Reef Bleaching: Facts, Hypotheses and Implications. *Global Change Biol.* **1996**, *2*, 495−509.

(3) Takahashi, S.; Whitney, S.; Itoh, S.; Maruyama, T.; Badger, M. Heat Stress Causes Inhibition of the de Novo Synthesis of Antenna Proteins and Potobleaching in Cultured *Symbiodinium*. *Proc. Natl. Acad. Sci. U.S.A.* **2008**, *105*, 4203−4208.

(4) Echigoya, R.; Rhodes, L.; Oshima, Y.; Satake, M. The Structures of Five New Antifungal and Hemolytic Amphidinol Analogs from Amphidinium carterae Collected in New Zealand. *Harmful Algae* **2005**, *4*, 383−389.

(5) Hofmann, E.; Wrench, P. M.; Sharples, F. P.; Hiller, R. G.; Welte, W.; Diederichs, K. Structural Basis of Light Harvesting by Carotenoids: Peridinin-Chlorophyll-Protein from *Amphidinium carterae*. *Science* **1996**, *272*, 1788−1791.

(6) Schulte, T.; Niedzwiedzki, D. M.; Birge, R. R.; Hiller, R. G.; Polivka, T.; Hofmann, E.; Frank, H. A. Identification of a Single Peridinin Sensing Chl-*a* Excitation in Reconstituted PCP by Crystallography and Spectroscopy. *Proc. Natl. Acad. Sci. U.S.A.* **2009**, *106*, 20764−20769.

(7) Schulte, T.; Johanning, S.; Hofmann, E. Structure and Function of Native and Refolded Peridinin-Chlorophyll-Proteins from Dinoflagellates. *Eur. J. Cell Biol.* **2010**, *89*, 990−997.

(8) Schulte, T.; Hiller, R. G.; Hofmann, E. X-ray Structures of the Peridinin-Chlorophyll-Protein Reconstituted with Different Chlorophylls. *FEBS Lett.* **2010**, *584*, 973−978.

(9) Ilagan, R. P.; Koscielecki, J. F.; Hiller, R. G.; Sharples, F. P.; Gibson, G. N.; Birge, R. R.; Frank, H. A. Femtosecond Time-Resolved Absorption Spectroscopy of Main-Form and High-Salt Peridinin-Chlorophyll *a*-Proteins at Low Temperatures. *Biochemistry* **2006**, *45*, 14052−14063.

(10) Ilagan, R. P.; Shima, S.; Melkozernov, A.; Lin, S.; Blankenship, R. E.; Sharples, F. P.; Hiller, R. G.; Birge, R. R.; Frank, H. A. Spectroscopic Properties of the Main-Form and High-Salt Peridinin-Chlorophyll *a* Proteins from *Amphidinium carterae*. *Biochemistry* **2004**, *43*, 1478−1487.

(11) Jiang, J.; Zhang, H.; Kang, Y.; Bina, D.; Lo, C. S.; Blankenship, R. E. Characterization of the Peridinin−Chlorophyll *a*-Protein Complex in the Dinoflagellate *Symbiodinium*. *Biochim. Biophys. Acta, Bioenerg.* **2012**, *1817*, 983−989.

(12) Niedzwiedzki, D. M.; Blankenship, R. E. Singlet and Triplet Excited State Properties of Natural Chlorophylls and Bacteriochlorophylls. *Photosynth. Res.* **2010**, *106*, 227−238.

(13) Niedzwiedzki, D. M.; Fuciman, M.; Frank, H. A.; Blankenship, R. E. Energy Transfer in an LH4-like Light Harvesting Complex from the Aerobic Purple Photosynthetic Bacterium *Roseobacter denitrificans*. *Biochim. Biophys. Acta, Bioenerg.* **2011**, *1807*, 518−528.

(14) van Stokkum, I. H.; Larsen, D. S.; van Grondelle, R. Global and Target Analysis of Time-Resolved Spectra. *Biochim. Biophys. Acta, Bioenerg.* **2004**, *1657*, 82−104.

(15) Zigmantas, D.; Polivka, T.; Hiller, R. G.; Yartsev, A.; Sundstrom, V. Spectroscopic and Dynamic Properties of the Peridinin Lowest Singlet Excited States. *J. Phys. Chem. A* **2001**, *105*, 10296−10306.

(16) Fuciman, M.; Enriquez, M. M.; Kaligotla, S.; Niedzwiedzki, D. M.; Kajikawa, T.; Aoki, K.; Katsumura, S.; Frank, H. A. Singlet and Triplet State Spectra and Dynamics of Structurally Modified Peridinins. *J. Phys. Chem. B* **2011**, *115*, 4436−4445.

(17) Polivka, T.; Hiller, R. G.; Frank, H. A. Spectroscopy of the Peridinin-Chlorophyll-*a* Protein: Insight into Light-Harvesting Strategy of Marine Algae. *Arch. Biochem. Biophys.* **2007**, *458*, 111−120.

(18) Kleima, F. J.; Wendling, M.; Hofmann, E.; Peterman, E. J. G.; van Grondelle, R.; van Amerongen, H. Peridinin Chlorophyll *a* Protein: Relating Structure and Steady-State Spectroscopy. *Biochemistry* **2000**, *39*, 5184−5195.

(19) Alexandre, M. T.; Luhrs, D. C.; van Stokkum, I. H.; Hiller, R.; Groot, M. L.; Kennis, J. T.; van Grondelle, R. Triplet State Dynamics in Peridinin-Chlorophyll-*a*-Protein: a New Pathway of Photoprotection in LHCs? *Biophys. J.* **2007**, *93*, 2118−2128.

(20) Carbonera, D.; Giacometti, G.; Segre, U.; Angerhofer, A.; Gross, U. Model for Triplet-Triplet Energy Transfer in Natural Clusters of Peridinin Molecules Contained in Dinoflagellate's Outer Antenna Proteins. *J. Phys. Chem. B* **1999**, *103*, 6357−6362.

(21) Mezzetti, A.; Spezia, R. Time-Resolved Step Scan FTIR Spectroscopy and DFT Investigation on Triplet Formation in Peridinin-Chlorophyll-a-Protein from *Amphidinium carterae* at Low Temperature. *Spectrosc. Int. J.* **2008**, *22*, 235−250.

(22) Bonetti, C.; Alexandre, M. T.; van Stokkum, I. H.; Hiller, R. G.; Groot, M. L.; van Grondelle, R.; Kennis, J. T. Identification of Excited-State Energy Transfer and Relaxation Pathways in the Peridinin-Chlorophyll Complex: an Ultrafast Mid-Infrared Study. *Phys. Chem. Chem. Phys.* **2010**, *12*, 9256−9266.

(23) Jeffrey, S. W.; Haxo, F. T. Photosynthetic Pigments of Symbiotic Dinoflagellates (Zooxanthellae) from Corals and Clams. *Biol. Bull.* **1968**, *135*, 149−165.

(24) Bowers, P. G.; Porter, G. Quantum Yields of Triplet Formation in Solutions of Chlorophyll. *Proc. R. Soc. London, Ser. A* **1967**, *296*, 435−441.

(25) Linden, P. A.; Zimmermann, J.; Brixner, T.; Holt, N. E.; Vaswani, H. M.; Hiller, R. G.; Fleming, G. R. Transient Absorption Study of Peridinin and Peridinin-Chlorophyll *a*-Protein after Two-Photon Excitation. *J. Phys. Chem. B* **2004**, *108*, 10340−10345.

(26) Bautista, J. A.; Hiller, R. G.; Sharples, F. P.; Gosztola, D.; Wasielewski, M.; Frank, H. A. Singlet and Triplet Energy Transfer in the Peridinin-Chlorophyll *a*-Protein from *Amphidinium carterae*. *J. Phys. Chem. A* **1999**, *103*, 2267−2273.

(27) van Stokkum, I. H. M.; Papagiannakis, E.; Vengris, M.; Salverda, J. M.; Polivka, T.; Zigmantas, D.; Larsen, D. S.; Lampoura, S. S.; Hiller, R. G.; van Grondelle, R. Inter-Pigment Interactions in the Peridinin Chlorophyll Protein Studied by Global and Target Analysis of Time Resolved Absorption Spectra. *Chem. Phys.* **2009**, *357*, 70−78.

(28) Krueger, B. P.; Lampoura, S. S.; van Stokkum, I. H.; Papagiannakis, E.; Salverda, J. M.; Gradinaru, C. C.; Rutkauskas, D.; Hiller, R. G.; van Grondelle, R. Energy Transfer in the Peridinin Chlorophyll-*a* Protein of *Amphidinium carterae* Studied by Polarized Transient Absorption and Target Analysis. *Biophys. J.* **2001**, *80*, 2843−2855.

(29) Zigmantas, D.; Hiller, R. G.; Sundstrom, V.; Polivka, T. Carotenoid to Chlorophyll Energy Transfer in the Peridinin-Chlorophyll-*a*-Protein Complex Involves an Intramolecular Charge Transfer State. *Proc. Natl. Acad. Sci. U.S.A.* **2002**, *99*, 16760−16765.

(30) Christensson, N.; Chabera, P.; Hiller, R. G.; Pullerits, T.; Polivka, T. Four-Wave-Mixing Spectroscopy of Peridinin in Solution

and in the Peridinin-Chlorophyll-*a* Protein. *Chem. Phys.* **2010**, *373*, 15−22.
(31) Shima, S.; Ilagan, R. P.; Gillespie, N.; Sommer, B. J.; Hiller, R. G.; Sharples, F. P.; Frank, H. A.; Birge, R. R. Two-Photon and Fluorescence Spectroscopy and the Effect of Environment on the Photochemical Properties of Peridinin in Solution and in the Peridinin-Chlorophyll-Protein from *Amphidinium carterae*. *J. Phys. Chem. A* **2003**, *107*, 8052−8066.
(32) Akimoto, S.; Takaichi, S.; Ogata, T.; Nishimura, Y.; Yamazaki, I.; Mimuro, M. Excitation Energy Transfer in Carotenoid-Chlorophyll Protein Complexes Probed by Femtosecond Fluorescence Decays. *Chem. Phys. Lett.* **1996**, *260*, 147−152.
(33) Kleima, F. J.; Hofmann, E.; Gobets, B.; van Stokkum, I. H. M.; van Grondelle, R.; Diederichs, K.; van Amerongen, H. Förster Excitation Energy Transfer in Peridinin-Chlorophyll-*a*-Protein. *Biophys. J.* **2000**, *78*, 344−353.
(34) Carbonera, D.; Giacometti, G.; Segre, U.; Hofmann, E.; Hiller, R. G. Structure-Based Calculations of the Optical Spectra of the Light-harvesting Peridinin-Chlorophyll-Protein Complexes from *Amphidinium carterae* and *Heterocapsa pygmaea*. *J. Phys. Chem. B* **1999**, *103*, 6349−6356.
(35) Damjanovic, A.; Ritz, T.; Schulten, K. Excitation Transfer in the Peridinin-Chlorophyll-Protein of *Amphidinium carterae*. *Biophys. J.* **2000**, *79*, 1695−1705.
(36) Vaswani, H. M.; Hsu, C. P.; Head-Gordon, M.; Fleming, G. R. Quantum Chemical Evidence for an Intramolecular Charge-Transfer State in the Carotenoid Peridinin of Peridinin-Chlorophyll-Protein. *J. Phys. Chem. B* **2003**, *107*, 7940−7946.
(37) Polivka, T.; Sundstrom, V. Ultrafast Dynamics of Carotenoid Excited States-from Solution to Natural and Artificial Systems. *Chem. Rev.* **2004**, *104*, 2021−2071.
(38) Di Valentin, M.; Ceola, S.; Salvadori, E.; Agostini, G.; Giacornetti, G. M.; Carbonera, D. Spectroscopic Properties of the Peridinins Involved in Chlorophyll Triplet Quenching in High-Salt Peridinin-Chlorophyll *a*-Protein from *Amphidinium carterae* as Revealed by Optically Detected Magnetic Resonance, Pulse EPR and Pulse ENDOR Spectroscopies. *Biochim. Biophys. Acta* **2008**, *1777*, 1355−1363.
(39) Carbonera, D.; Giacometti, G.; Segre, U. Carotenoid Interactions in Peridinin Chlorophyll *a* Proteins from Dinoflagellates - Evidence for Optical Excitons and Triplet Migration. *J. Chem. Soc., Faraday Trans.* **1996**, *92*, 989−993.
(40) Di Valentin, M.; Ceola, S.; Salvadori, E.; Agostini, G.; Carbonera, D. Identification by Time-Resolved EPR of the Peridinins Directly Involved in Chlorophyll Triplet Quenching in the Peridinin-Chlorophyll *a*-Protein from *Amphidinium carterae*. *Biochim. Biophys. Acta* **2008**, *1777*, 186−195.
(41) Di Valentin, M.; Ceola, S.; Agostini, G.; Giacometti, G. M.; Angerhofer, A.; Crescenzi, O.; Barone, V.; Carbonera, D. Pulse ENDOR and Density Functional Theory on the Peridinin Triplet State Involved in the Photo-Protective Mechanism in the Peridinin-Chlorophyll a-Protein from Amphidinium carterae. *Biochim. Biophys. Acta, Bioenerg.* **2008**, *1777*, 295−307.
(42) Di Valentin, M.; Tait, C.; Salvadori, E.; Ceola, S.; Scheer, H.; Hiller, R. G.; Carbonera, D. Conservation of Spin Polarization during Triplet-Triplet Energy Transfer in Reconstituted Peridinin-Chlorophyll-Protein Complexes. *J. Phys. Chem. B* **2011**, *115*, 13371−13380.
(43) Schödel, R.; Irrgang, K. D.; Voigt, J.; Renger, G. Rate of Carotenoid Triplet Formation in Solubilized Light-Harvesting Complex II (LHCII) from Spinach. *Biophys. J.* **1998**, *75*, 3143−3153.
(44) Polivka, T.; Pascher, T.; Sundstrom, V.; Hiller, R. G. Tuning Energy Transfer in the Peridinin-Chlorophyll Complex by Reconstitution with Different Chlorophylls. *Photosynth. Res.* **2005**, *86*, 217−227.
(45) Niklas, J.; Schulte, T.; Prakash, S.; van Gastel, M.; Hofmann, E.; Lubitz, W. Spin-Density Distribution of the Carotenoid Triplet State in the Peridinin-Chlorophyll-Protein Antenna. A Q-Band Pulse Electron-Nuclear Double Resonance and Density Functional Theory Study. *J. Am. Chem. Soc.* **2007**, *129*, 15442−15443.
(46) Bonetti, C.; Alexandre, M. T. A.; Hiller, R. G.; Kennis, J. T. M.; van Grondelle, R. Chl-*a* Triplet Quenching by Peridinin in H-PCP and Organic Solvent Revealed by Step-Scan FTIR Time-Resolved Spectroscopy. *Chem. Phys.* **2009**, *357*, 63−69.
(47) Gall, A.; Berera, R.; Alexandre, M. T. A.; Pascal, A. A.; Bordes, L.; Mendes-Pinto, M. M.; Andrianambinintsoa, S.; Stoitchkova, K. V.; Marin, A.; Valkunas, L.; et al. Molecular Adaptation of Photoprotection: Triplet States in Light-Harvesting Proteins. *Biophys. J.* **2011**, *101*, 934−942.
(48) Angerhofer, A.; Bornhauser, F.; Gall, A.; Cogdell, R. J. Optical and Optically Detected Magnetic-Resonance Investigation on Purple Photosynthetic Bacterial Antenna Complexes. *Chem. Phys.* **1995**, *194*, 259−274.
(49) Niyogi, K. K. Photoprotection Revisited: Genetic and Molecular Approaches. *Annu. Rev. Plant Physiol.* **1999**, *50*, 333−359.
(50) Krieger-Liszkay, A. Singlet Oxygen Production in Photosynthesis. *J. Exp. Bot.* **2005**, *56*, 337−346.
(51) Foote, C. S. Photosensitized Oxidation and Singlet Oxygen: Consequences in Biological Systems. In *Free Radicals in Biology*; Pryor, W.A., Ed.; Academic Press: New York, 1976; pp 85−133.